JYX JYVÄSKYLÄN YLIOPISTO UNIVERSITY OF JYVÄSKYLÄ

This is a self-archived version of an original article. This version may differ from the original in pagination and typographic details.

Author(s): Niskanen, Joni; Lahtinen, Manu; Perämäki, Siiri

Title: Acetic acid leaching of neodymium magnets and iron separation by simple oxidative precipitation

Year: 2022

Version: Published version

Copyright: © 2022 the Authors

Rights: CC BY 4.0

Rights url: https://creativecommons.org/licenses/by/4.0/

Please cite the original version:

Niskanen, J., Lahtinen, M., & Perämäki, S. (2022). Acetic acid leaching of neodymium magnets and iron separation by simple oxidative precipitation. Cleaner Engineering and Technology, 10, Article 100544. https://doi.org/10.1016/j.clet.2022.100544

Cleaner Engineering and Technology 10 (2022) 100544

Contents lists available at ScienceDirect

Cleaner Engineering and Technology

journal homepage: www.sciencedirect.com/journal/cleaner-engineering-and-technology

Acetic acid leaching of neodymium magnets and iron separation by simple oxidative precipitation

Joni Niskanen *, Manu Lahtinen, Siiri Perämäki

Department of Chemistry, University of Jyväskylä, Finland

ARTICLE INFO

Keywords:
Spent NdFeB magnet
Rare earth element
REE
Critical raw material
Acetic acid leaching
Iron precipitation

ABSTRACT

Neodymium-iron-boron (NdFeB) has become the most prominent permanent magnet alloy, with a wide variety of applications and an ever-increasing demand. Their recycling is important for securing the supply of critical raw materials used in their manufacturing. The use of organic acids such as acetic acid has been of recent interest for the recycling of waste NdFeB magnets. Despite achieving good leaching efficiencies, the published literature has not properly investigated the effects of key factors influencing the acetic acid leaching process and their respective interactions, which has led to conflicting findings as to what conditions are optimal. The present work goes to show that no such optimum exists by taking a look at the major factors (concentration, solid-to-liquid ratio, time, and temperature) and their interactions. The results show that leaching efficiencies >95% and even up to 100% can be achieved using a variety of different conditions showing that the leaching reaction is quite flexible, which is helpful for a potential upscaling of the process. The separation of the leached elements presents another problem in NdFeB magnet processing. As a novel application, this work investigated iron separation from the acetic acid leachate by the means of simple and inexpensive aeration. It was found that up to 99% of iron could be precipitated as FeO(OH) (goethite) within 2 h at pH 5 and 80 °C, while only minor neodymium co-precipitation was observed (5%). Separation of iron from the leachate can help obtain purer REE products in further processing.

1. Introduction

Since their development in the 1980s, neodymium permanent magnets (NdFeB) have become key components in many applications and electronic devices. Far superior to other magnetic materials in most respects — having higher remanence, coercivity, and energy product, but lower Curie temperature — NdFeB magnets have replaced samarium-cobalt, alnico, and ferrite magnets in many applications (Cullity and Graham, 2009). A number of other elements (Al, Co, Dy, Ni, Pr, Tb) can be added to the alloy to improve some of its properties, e.g., useable temperature range (Brown et al., 2002). NdFeB magnets are commonly found in computer and office automation, automotive parts, consumer electronics and appliances, industrial automation, and other high-tech applications (Gislev and Grohol, 2018).

Ever increasing global adoption and use of various electronic devices and their eventual discarding has caused an increase in the generation of waste electronic and electrical equipment (WEEE or e-waste). It is estimated they already constituted roughly 8% of municipal waste with 41.8 Mt of e-waste produced in 2014 (Kaya 2019). Global e-waste generation has seen a substantial increase since, reaching 53.6 Mt in 2019 (excluding photovoltaics), and is estimated to exceed 74 Mt in 2030 (Forti et al., 2020).

Two-thirds of NdFeB magnets are used in computers, wind turbines, and automotive applications (Rademaker et al., 2013), which also represent areas with great potential for growth. A 2018 report by the European Commission estimates that the demand for neodymium, praseodymium, and dysprosium in wind power applications in the EU could increase as much as 40-fold come 2030 compared with 2015, assuming the European Wind Energy Association's high estimate of the total wind power production of 988 TW h, equal to 31% of EU electricity demand in 2030 (Corbetta 2015). Similarly, expanding electric vehicle production is estimated to need 10 times as much Nd, Pr, and Dy in 2030 compared with 2015 values. Even the lower estimates for wind power expansion place their combined annual raw material demands at 2000 t of Nd and 500 t of both Pr and Dy.

This rapid growth poses a serious issue when it comes to disposal, and maybe even more importantly supply security, as most of the world's virgin rare earth element (REE) production — including that of

* Corresponding author.
E-mail address: joni.m.niskanen@jyu.fi (J. Niskanen).

https://doi.org/10.1016/j.clet.2022.100544
Received 21 March 2022; Received in revised form 24 May 2022; Accepted 1 August 2022
Available online 9 August 2022
2666-7908/© 2022 The Authors. Published by Elsevier Ltd. This is an open access article under the CC BY license (http://creativecommons.org/licenses/by/4.0/).

Nd, Pr, and Dy — is concentrated in China. E-waste presents a potential secondary source for raw material production. Current recycling efforts satisfy 6–7% of the REE demand in the EU. A ramp-up in recycling could result in an annual neodymium production of over 400 t come 2030, but with rapidly increasing demand, this would still satisfy only about 8% of Nd demand, depending on the estimates. Globally recycling is estimated to produce over 2200 t of Nd and cover 9% of the demand in 2030.

The mounting pressure for the recycling of REE-containing waste sources, like that of NdFeB magnets, has prompted the scientific community to find novel solutions for their processing. Some emphasis has to be placed on finding low-cost approaches in addition to novelty, for any NdFeB recycling process has to compete with virgin raw material production. The price of neodymium oxide has been quite steady, approximately 40 € kg^{-1} for the past few years (Mineral Commodity Summaries 2021), setting a benchmark for any NdFeB magnet recycling process development for the time being. REE prices are expected to rise as demand increases, but increasing prices are also expected to prompt the opening of new mines and increase the size of estimated reserves (Habib and Wenzel, 2014), curbing expectations for future price hikes.

Recycling and reprocessing of waste NdFeB magnets have been studied intensely in the past two decades with a wide variety of approaches taken (Yang et al., 2017). Direct recycling methods include re-sintering, melt spinning, hydrogen decrepitation deabsorbation recombination (HDDR), and recasting, but the variation between different alloys and their composition, in addition to the lower quality products obtained by direct recycling methods, makes it impractical in most cases and metallurgical processes more appealing. Metallurgical processes are divided into pyrometallurgical and hydrometallurgical routes. The former includes methods such as oxidative roasting (Firdaus et al., 2016) and selective chlorination (Itoh et al., 2008). The latter usually consists of a leaching step, using one of many possible leaching methods, followed by one or more metal recovery steps, employing processes such as precipitation, ion exchange, solvent extraction, and electrochemical methods (Binnemans et al., 2013).

Conventional leaching processes commonly employ mineral acids, but other leaching methods have been pursued in the past few years. These novel approaches include the use of ionic liquids (IL), which can be useful in both the leaching of NdFeB magnets (Orefice et al., 2018) and the metals extraction step when leaching with acids (Riaño and Binnemans, 2015). Another novel line of research is the use of organic acids, which is also in line with the principles of green chemistry (Sáenz-Galindo et al., 2021), contributing to their appeal. A variety of organic acids have been studied for use in the leaching of spent NdFeB magnets, such as acetic, ascorbic, citric, formic, glycolic, maleic, malic, oxalic and tartaric acids. Similar efforts have been undertaken for the leaching of lithium-ion battery wastes (Li et al., 2013). Many of the studied organic acids seem viable for use as a leaching agent, but acetic acid appears more appealing due to its lower production cost. Acetic acid has the added benefit of being able to be produced entirely via renewable biological processes such as the oxidative fermentation of ethanol or anaerobic fermentation of sugars, and some bacteria are even able to produce acetic acid from one-carbon compounds like carbon monoxide, all of which have the advantage of low energy and raw material costs (Sim et al., 2007).

One of the challenges in the hydrometallurgical processing of spent NdFeB magnets is the extraction and production of pure REE products, for the high iron concentration in NdFeB leach liquors is known to cause problems and result in impurities when using some common REE separation methods, such as liquid-liquid extraction (Parhi et al., 2016) or the oxalate precipitation method (Liu et al., 2020a, 2020b). This problem may be resolved by using the oxidative roasting–selective leaching method (Liu et al., 2020a, 2020b) or by separating iron prior to REE recovery, e.g., by hydroxide addition (Önal et al., 2017). Another conventional method for iron separation from an aqueous media is oxidation and precipitation of iron (Free 2013), which has been employed in the treatment of e.g. ground waters, estuaries, and hydrometallurgical wastewaters. Iron(II) is readily oxidised to iron(III) when exposed to air or a number of other oxidising agents, although the rate of air oxidation is slow in acidic solutions, becoming more rapid as pH increases (Kroschwitz et al., 2001). Possible oxidants include air (aeration), NH_2OH, NaOCl, $KMnO_4$, H_2O_2, Cl_2, O_3, ClO_2 and MnO_2 (Khatri et al., 2017), of which aeration, hydrogen peroxide and ozone carry the benefit of not introducing extra elements into the solution, making further processing that much easier.

Recycling of NdFeB magnets and REE recovery has been of great interest in this millennium. In addition to conventional hydrometallurgical processing using mineral acids, the use of organic acids has garnered some attention as an application of green chemistry principles. Acetic acid is one of the prime candidates and has been the subject of some previous work. It has been successfully utilised in the leaching of powdered NdFeB magnets as is (Behera and Parhi 2016). The use of auxiliary techniques like ultrasound and microwave can be used to speed up the process (Behera et al., 2019). While achieving high leaching efficiencies (99.99%), the previous work has not properly examined the effects of individual factors and their interactions for they have been conducted using the one-factor-at-a-time (OFAT) method. The OFAT method suffers from an inability to detect and estimate possible interactions between the different factors and as a result, can miss the optimal conditions, should they exist in the first place. In this work, a multivariate analysis of the most prominent factors influencing the leaching reaction — concentration, solid-to-liquid ratio, time and temperature — is performed by employing a 2-level full factorial experimental design, which allows for estimation of the effects of individual factors independently and their respective interactions.

A major complication in any hydrometallurgical process is the separation of leached elements. In the case of NdFeB processing and acetic acid leaching, the previous work has attempted iron separation by the means of oxidative roasting and selective leaching. At best the production of insoluble iron oxides and soluble REE oxides has resulted in a fairly high separation of iron (99.0%) and Nd recovery (94.2%) (Yoon et al., 2015), while others have not managed such good separation (21–38%) and have relied on solvent extraction for further separation (Gergoric et al., 2018). The very high temperatures and energy intensity of the roasting process can be considered a downside. Instead of selective leaching, separation of iron from the leachate can be achieved via the oxidative precipitation of iron. Used in many other applications (Khatri et al., 2017), the method sees its novel application in the hydrometallurgical processing of NdFeB magnets. The present work investigates a few oxidation methods (air, H_2O_2) and the effect of the primary factors influencing the precipitation reaction (pH, T and t), showing that it is a feasible alternative for iron separation.

2. Experimental

2.1. Materials

Spent NdFeB magnets from manually disassembled hard disk drives (HDD) — received from a Finnish recycling company Green Disposal Oy, Ltd — were demagnetized in a muffle furnace at a temperature of 400 °C for 3 h. Magnets were manually crushed with a setup resembling mortar and pestle and passed through a 500 μm sieve to obtain a fine powder, which was used throughout the study.

Glacial acetic acid (100%, VWR AnalaR NORMAPUR ACS) diluted to specified concentrations was used for all of the leaching experiments. Water used for dilutions, washing, etc. was ultra-pure grade (Merck Millipore Milli-Q, Germany), and herein referred to as just water. Concentrated nitric acid (>65%, Honeywell Fluka) was used to prepare 5% nitric acid solutions, which in turn were used for the preparation and dilution of both standard and sample solutions for inductively coupled plasma-optical emission spectroscopy (ICP-OES). In the iron precipitation experiments, a hydrogen peroxide solution (33%, VWR) was used as an oxidiser, and a sodium hydroxide solution (50%, J.T.Baker) diluted to

5% was used for pH adjustment. Filtration was performed using Whatman filter papers.

2.2. Analytical methods

Elemental analysis of the pretreated sample material was carried out by total acid digestion using aqua regia, and a subsequent determination of Al, B, Co, Dy, Fe, Nd, Ni, Pr, and Tb concentrations in the sample solutions by inductively coupled plasma-optical emission spectroscopy (ICP-OES, Perkin Elmer Avio 500, USA). The magnet powder was examined with a scanning electron microscope (SEM, Zeiss EVO-50XVP, Germany) fitted with an energy-dispersive X-ray detector (EDS, Bruker Quantax 400, USA), which was utilised for semi-quantitative elemental analyses. Sample solutions obtained from the leaching and iron precipitation experiments were analysed with ICP-OES to measure elemental concentrations to determine leaching and precipitation efficiencies. The particle size distribution of the magnet powder was analysed with a laser diffraction particle size analyser (Malvern Mastersizer 3000, UK) fitted with a Hydro MV dispersion unit. Samples were suspended in deionized water and ultrasound was applied during measurement to break down agglomerates. Analysis was performed in triplicate and the Fraunhofer scattering model was used for particle size estimation.

The elemental composition of the iron precipitate was determined using ICP-OES and SEM-EDS. Additionally, a powder x-ray diffractometer (PXRD, Malvern Panalytical X'Pert PRO, United Kingdom) with Cu K_α radiation ($\lambda = 0.154187$ nm, generated by sealed X-ray tube and Ni β-filter; 45 kV, 40 mA) was used to identify the major crystalline phases of the iron precipitate. Each lightly hand-ground sample was attached onto a steel-made sample holder with a 16 mm diameter sample cavity. Diffraction intensities were recorded by an X'Celerator detector at room temperature from a spinning sample with a 2θ–range of 6–90°, a step size of 0.017∘ and counting times of 180 s per step (overall time of a scan 2 h). Data processing and search-match phase analyses were carried out by program X'Pert HighScore Plus (v. 4.9) (Degen et al., 2014) and ICDD PDF4+ database (Gates-Rector and Blanton, 2019).

2.3. Acetic acid leaching

2.3.1. Initial experiments

Leaching of the magnet powder was initially tested by conducting three experiments with duplicate samples and leaching at three different acetic acid concentration levels (0.4, 0.7 and 1.0 mol L^{-1}), all using a 1 g per 100 ml S/L ratio. Further two experiments were run using two different, lower S/L ratios (1 g per 150 ml and 1 g per 200 ml), leaching with 1 mol L^{-1} acid solution. Experiments were conducted in 250 ml beakers, leaching for 24 h at 20 °C and stirring at 600 min^{-1} on a hotplate stirrer (Heidolph MR Hei-Tec, Germany). Afterwards, the sample solutions were filtered through paper filters into volumetric flasks and filled with water. The samples were further diluted with a 5% HNO_3 solution prior to ICP-OES measurement.

Leaching efficiencies for each element (x) were calculated by comparing the values obtained from ICP-OES to ones calculated from sample mass and the pre-determined mass fractions of the sample material:

$$\text{Leaching efficiency} = \frac{c_{x,\ \text{measured}} \times V_{\text{initial}} \times \text{dilution}}{m_{\text{sample}} \times \text{wt.}\%_x} \quad (1)$$

2.4. Main effects and interactions

The effect of different factors (concentration, solid-to-liquid ratio, temperature and time) on acetic acid leaching efficiency was studied by conducting a series of leaching experiments, which were performed in 50 ml plastic screw cap test tubes in a covered water bath, heated and stirred with a magnetic stirrer hotplate. Leachant was preheated to the desired temperature prior to leaching, the temperature of the bath was adjusted to 20,50 and 80 °C and monitored with a mercury-in-glass thermometer, and the stirrer was set to 600 min^{-1}. Leachant volume was kept constant (50 ml) and the S/L ratio varied by varying sample mass. Leaching solutions were then filtered, transferred into volumetric flasks and filled with water, and further diluted with a 5% HNO_3 solution for ICP-OES analysis.

Table 1
The four factors and their respective levels selected for the 2-level full factorial experimental design, including a centre point.

Factor/Level	Lower	Centre	Upper
Concentration (mol L^{-1})	0.2	0.6	1.0
S/L ratio (g mL^{-1})	1/150	1/75	1/50
Temperature (°C)	20	50	80
Time (h)	1	3.5	6

To assess the individual effects of each factor and their respective interactions, experimental design (DOE) was used for the experiment. A 2-level full factorial randomized design with a centre point triplicate was employed to gain insight into the general direction and amplitude of the effects and possible curvature of response. The R software environment (R version 4.0.2 with Rcmdr 2.7-1 and RcmdrPlugin.DoE 0.12–3 and their dependencies) was used for creating the design and analysing the results. The selection of factors and their respective levels — presented in Table 1 — was based on existing literature and our own initial experiments.

2.5. Leaching kinetics

Kinetics of the acetic acid leaching was studied in select conditions employing 2 series of triplicate sample solutions. 2 g of the magnet powder was leached in a covered 400 ml beaker using 200 ml of 0.4 mol L^{-1} acetic acid solution at a temperature of 20 °C on a magnetic stirrer set to 600 min^{-1}. Periodical subsamples (V =0.5 ml) were taken with an automatic pipette, filtered through a paper filter, filters washed with water and sample immediately diluted with 5% HNO_3 for ICP-OES analysis. Stirring was halted, and solids were allowed to settle for 1 min each time before sampling. For the first series, subsamples were taken after 1, 2, 3, 4, 5, 6, 7, 8, 12 and 24 h of leaching, and for the second series after 16, 20, 24 and 40 h.

2.6. Iron precipitation

Pregnant leaching solutions (PLS) for the iron precipitation experiments were prepared by dissolving the powdered magnets using a 0.4 mol L^{-1} acetic acid solution and an S/L ratio of 1/150 g mL^{-1} and leaching for 24 h at 20 °C to ensure complete dissolution.

Precipitation experiments were carried out in 250 ml beakers placed on magnetic stirrer hotplates. The stirrer speed was set to 800 min^{-1} and the temperature of the sample solutions was monitored using an external probe submerged in the solution, which controlled the hotplate. The pH of the samples was monitored using a pH meter (Mettler Toledo SevenEasy pH with InLab Expert NTC30 pH electrode, USA) and adjusted using a diluted sodium hydroxide solution. Precipitation of the dissolved iron was achieved by oxidation of Fe^{2+} ions to Fe^{3+} ions, and facilitated using three different methods: 1) ambient air/oxygen dissolution, 2) direct air feed/aeration and 3) hydrogen peroxide addition. Sample solutions were transferred into 50 ml centrifuge tubes afterwards and the precipitate was separated by centrifuging at 3500 min^{-1} for 5 min, after which the resulting supernatant was carefully removed using a pipette.

The composition of the precipitate was determined after the precipitation experiments by preparing three replicate samples. PLS were prepared as described at the beginning of this section (2.4) and precipitation was conducted at 90 °C and pH 5, stirring at 800 min^{-1} and

Table 2
Elemental composition (wt.%) of the magnet as determined quantitatively by ICP-OES and semi-quantitatively by SEM-EDS. Dysprosium was unable to be determined with EDS due to overlapping peaks of Fe and Dy, and boron due to the use of a boron viewing window.

	Fe	Nd	Pr	Ni	Dy	Co	B	Al	Tb	O	C	Σ
ICP-OES	64.45	24.94	3.63	2.55	1.34	1.12	1.06	0.57	0.19	–	–	99.86
SEM-EDS	61.08	27.63	4.49	0.20	–	1.78	–	0.48	0.00	3.24	1.10	100.00

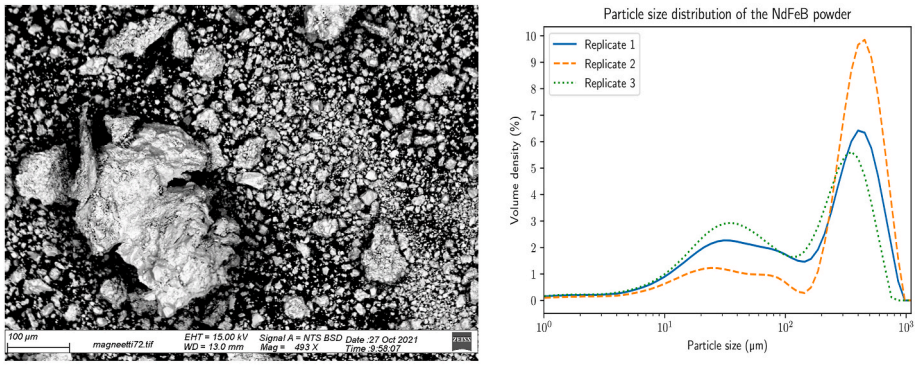

(a) (b)

Fig. 1. (a) SEM image of the magnet powder captured with the back-scattered electron detector. (b) Particle size distribution of the magnet powder.

allowing 2 h to react. The formed precipitates were separated by centrifugation and the resulting supernatants were analysed with ICP-OES. Precipitates were dried overnight in an oven at 115 °C and the obtained powders were analysed with XRD and SEM-EDS. A portion of the precipitate was dissolved in aqua regia and analysed with ICP-OES.

Iron precipitation efficiencies were calculated assuming complete dissolution of the sample material, using the pre-determined mass fractions and comparing them with values obtained from ICP-OES:

$$\text{Precipitation efficiency} = 1 - \frac{c_{\text{measured}} \times V_{\text{initial}} \times \text{dilution}}{m_{\text{sample}} \times \text{wt.}\%_{\text{Fe}}} \quad (2)$$

3. Results and discussion

3.1. Analysis of sample material

Elemental concentrations of the sample material determined with ICP-OES and SEM-EDS are presented in Table 2. Results from the ICP-OES and EDS analyses appear to be in reasonably close agreement, although EDS results (see SI 1 for details) should be regarded as semi-quantitative. The obtained results correspond fairly well with theoretical values for a pure $Nd_2Fe_{14}B$ alloy (72% Fe, 27% Nd, 1% B) and those reported in the literature (59–65% Fe, 25–32% Nd, 0.66–1.26% B). The variation reported in these values may be explained by differing manufacturing processes, the inclusion of various additives and the use of different coating materials. Praseodymium can substitute neodymium to a certain degree, and it is used due to its lower cost (Rademaker et al., 2013). Aluminium, cobalt, dysprosium and terbium on the other hand may be added to improve certain properties of the alloy (Sagawa et al., 1987; Cullity and Graham, 2009; Brown et al., 2002; Rademaker et al., 2013). Nickel and zinc, among other materials, are commonly used as a protective coating, for sintered NdFeB magnets are prone to corrosion (Brown et al., 2002). The small amount of oxygen detected with EDS is likely due to ambient oxidation of the magnet powder. An SEM image of the magnet powder is shown in Fig. 1a. The image shows a fair amount of variability in particle size, ranging from only a few micrometres up to hundreds of micrometres in diameter. The particle size distributions obtained from the laser diffraction analysis (see SI 2 for details) is presented in Fig. 1b. The graph shows a large peak in the range of 200–900 µm for each sample and a smaller peak around 10–100 µm. 90% of the particles are <600 µm in size and 50% are <220 µm. The De Brouckere mean diameter ($D[4,3]$) of the three samples is 261 µm.

3.2. Leaching experiments

3.2.1. Initial experiments

The leaching reaction (Liu et al., 2020) for the neodymium magnet alloy —

$$REE_2Fe_{14}B(s) + 37H^+(aq) \longrightarrow 2REE^{3+}(aq) + 14Fe^{2+}(aq) + B^{3+}(aq) + 18\frac{1}{2}H_2(g) \quad (3)$$

— sets some constraints on the possible combinations of acetic acid concentration and solid-to-liquid ratio when the complete dissolution of the alloy is desired. Literature suggested that the leaching process benefits from low S/L ratios (Yoon et al., 2015; Behera and Parhi 2016), especially in the case of iron (Gergoric et al., 2018). An S/L ratio of 1 g per 100 mol L^{-1} was selected as a basis for the initial experiments. Based on Equation (3) it was calculated that a 0.34 mol L^{-1} acetic acid solution would be required at minimum to dissolve 1 g of the alloy. To maintain sufficient acidity of the solution and to prevent premature precipitation of the leached metals, a minimum concentration of 0.4 mol L^{-1} was selected for the experiment.

Table 3
Comparison of the reported leaching conditions for the acetic acid leaching of NdFeB magnet powders and the achieved leaching efficiencies.

Reference	Particle size (μm)	c_{AcH} (mol L^{-1})	S/L ratio/ pulp density	T (°C)	t (h)	ω (min^{-1})	LE Nd (%)
Yoon et al. (2015)	NT	1.0	1%	90	3	400	94.2
Behera and Parhi (2016)	106–150	0.4	1% (w/v)	80	4	800	>99.99
Gergoric et al. (2018)	<355	1.0	1/30–1/80 g mL^{-1}	25	24	400	>95
Erust et al. (2021)	<500	3	20 g L^{-1}	27	5	200	50

The initial leaching experiments (0.4, 0.7 and 1.0 mol L^{-1}) achieved mean Nd leaching efficiencies of 98, 96 and 95% respectively. Increasing acid concentration did not have much of an effect on leaching efficiency, confirming the hypothesis of 0.4 mol L^{-1} being sufficient when using an S/L ratio of 1 g per 100 ml and given enough time. The following two experiments with lower S/L ratios (1/150 and 1/200 g mL^{-1}) both reached 100% Nd dissolution, affirming that the reaction benefits from lower S/L ratios. The increase in leaching efficiency with decreasing S/L ratio is due to more protons (in absolute terms) being available for the leaching reaction within the solution because weak acids like acetic acid only dissociate partially in an aqueous solution. Using a higher S/L ratio (or lower concentration) can cause proton starvation in the leachate (Gergoric et al., 2018). Other explanations include increased surface area towards the leachant, and lower viscosity (Behera and Parhi 2016).

These findings affirm the general notion of dilute acetic acid being suitable for NdFeB magnet leaching in the right conditions. Table 3 lists the leaching efficiencies reported in the existing literature along with their respective leaching conditions. Yoon et al. (2015) focused on the grinding and roasting processes and did not study the leaching process itself in detail. Behera and Parhi (2016) performed a detailed kinetics study and reached virtually quantitative leaching efficiencies, but the study was conducted one factor at a time. Gergoric et al. (2018) carried out a similar OFAT study for leaching roasted NdFeB powders, albeit with fewer variables and lesser focus on the kinetics, but complemented with solvent extraction experiments. Erust et al. (2021) tested a variety of acids followed by a solvent extraction step using an ionic liquid, but placed very little emphasis on studying the leaching conditions and reported quite low leaching efficiencies for acetic acid, which might have been due to the high S/L ratio, low temperature, short leaching time or low stirring speed. The previous work has not taken into consideration the interfactor interactions and has not assessed the effect of each variable independent of the others. High leaching efficiencies have been reached using a variety of leaching conditions, which indicates that no global optimum exists. The initial tests and previous work show that the reaction is quite flexible, and complete dissolution of neodymium is possible using a variety of different leaching conditions, for which reason experimental design was employed for the following set of experiments to gain better insight into the effect of each variable independently as well as their respective interactions.

3.3. Main effects and interactions

Results obtained from ICP-OES measurements were used to calculate the leaching efficiencies of iron and neodymium for each experiment, and they are displayed in Table 4 alongside their respective leaching conditions. At a glance, the results reveal that very good leaching efficiencies (>95%) are attainable using a variety of different leaching conditions. They also confirm our assessment of concentrations lower than 0.4 mol L^{-1} being too low (sub-stoichiometric) when the S/L ratio is 1/100 or higher. However, a concentration as low as 0.2 mol L^{-1} appears entirely adequate when the S/L ratio is low enough. For visualisation of the results, the R software environment was used to draw main effects plots (Fig. 2a) and interaction plots (Fig. 2b) for the factors influencing neodymium leaching recovery. ANOVA was used to determine the statistical significance of the interactions, wherein the centre point replicates were used for the estimation of random error ($s^2 = 0.47$). It was found that all of the 2-way interactions were statistically significant, excluding $c - t$ and $S/L - t$, which displayed no interaction whatsoever. The 3-way interactions, excluding $c - S/L - t$, appeared statistically significant as well (see SI 3).

Using the included centre point to plot the response over the diagonals of the experimental design (see SI 4) shows that the response behaves quadratically. The centre point itself produced particularly good leaching efficiencies (95%), and very little gains are made by further adjustment of the individual factors towards the favourable directions seen in the main effects plot (Fig. 2a). Individual factors can also

Table 4
The full randomised 2-level factorial design generated using the values from Table 1, complete with the experimental results. Iron and neodymium leaching efficiencies are displayed alongside their respective leaching conditions.

Sample ID	Run order	Concentration (mol L^{-1})	S/L ratio (g mL^{-1})	Time (h)	Temperature (°C)	Leaching efficiency Fe (%)	Nd (%)
1	1	0.2	1/150	1	20	11.20	22.33
2	12	1.0	1/150	1	20	12.33	24.51
3	14	0.2	1/50	1	20	9.36	21.86
4	4	1.0	1/50	1	20	11.62	24.48
5	8	0.2	1/150	6	20	46.73	55.19
6	11	1.0	1/150	6	20	54.04	60.52
7	6	0.2	1/50	6	20	28.34	38.29
8	15	1.0	1/50	6	20	47.44	55.21
9	3	0.2	1/150	1	80	91.61	93.91
10	13	1.0	1/150	1	80	100.00	100.00
11	9	0.2	1/50	1	80	28.85	44.24
12	7	1.0	1/50	1	80	98.27	96.92
13	16	0.2	1/150	6	80	97.50	99.07
14	10	1.0	1/150	6	80	100.00	100.00
15	2	0.2	1/50	6	80	23.27	64.69
16	5	1.0	1/50	6	80	97.73	100.00
17	17	0.6	1/75	3.5	50	98.08	96.00
18	18	0.6	1/75	3.5	50	96.78	94.66
19	19	0.6	1/75	3.5	50	98.20	95.59

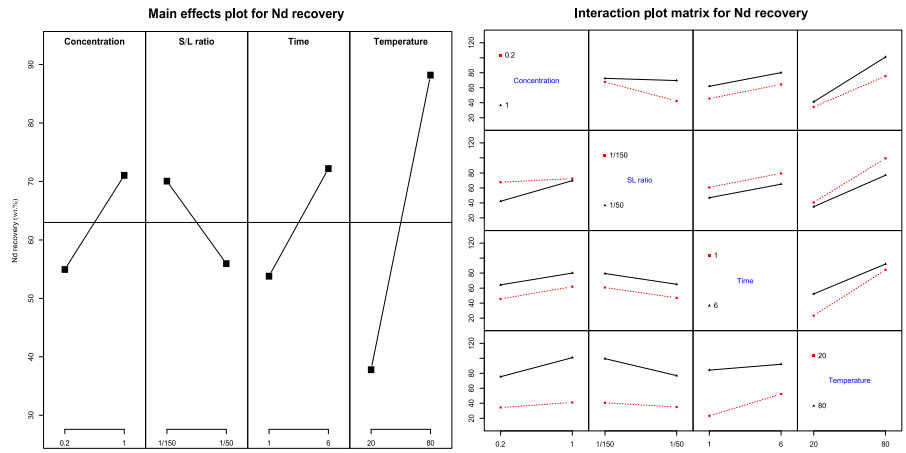

(a) (b)

Fig. 2. **(a)** The main effects plot, displaying the mean responses of each factor at their low and high settings, and the effect of changing each factor on average. **(b)** The interaction plot matrix, showing the average effect each variable had, respective to each other factor. The parallelity of lines within a single subplot indicates a lack of interaction between the two variables while converging lines are evidence of a possible interaction.

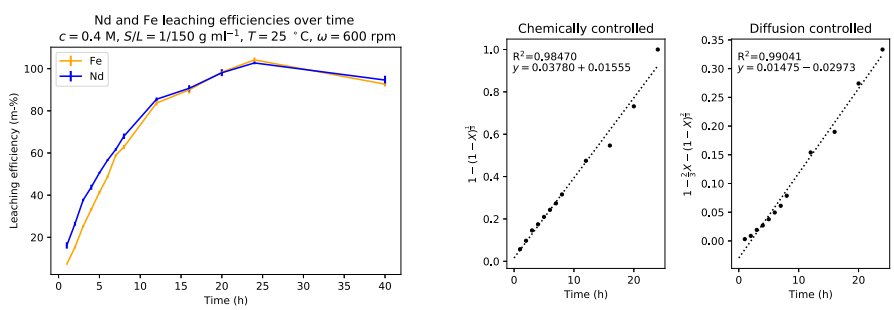

(a) (b)

Fig. 3. **(a)** Averages of the determined leaching efficiencies from the triplicate samples for both iron and neodymium plotted as a function of time. **(b)** Plots and linear fits for shrinking sphere/chemically controlled (left) and shrinking core/diffusion controlled (right) models using the data from the leaching experiment up to the 24 h mark.

be adjusted towards the unfavourable direction in some cases, as long as others are adjusted to compensate for that. Adjusting multiple factors in the unfavourable direction can have a dramatic negative effect, however. A discussion of these interactions follows.

The main effects plot shows that increasing concentration from 0.2 to 1.0 mol L^{-1} increased Nd recovery by 16 percentage points (pp) on average, and the interactions plot shows that it was significantly higher when the S/L ratio was high, which is a clear indication of the interconnected nature of the two factors. The interaction between concentration and S/L ratio is further exemplified by the interaction plots. When the S/L ratio is low, the mean effect of increasing concentration is a mere 5 pp when at a high S/L ratio it is 27 pp. The interaction is taken as the mean of their difference, giving a value of 11 pp, meaning that the effect of increasing concentration grows with increasing S/L ratio.

Similar conclusions can be drawn from the S/L plots, displaying an average decrease of 14 pp with an increasing S/L ratio. The highest reductions appeared when concentration was low, but virtually no change was observed when it was high. This is due to the aforementioned fact that there is not enough acid and protons present for complete dissolution to occur when the concentration is low and the S/L ratio is high. This phenomenon can also be understood through the acid to alloy molar ratio. As was shown in Equation (3), each mole of the alloy would theoretically require 37 mol of protons to achieve complete dissolution. At low concentration and high S/L ratio the molar ratio is roughly 11, which indeed is too low, but increasing just the S/L ratio brings the molar ratio up to 32. At the high concentration, the molar ratios are 54 and 162 respectively. The results show that lower acid concentrations can be compensated for with lower S/L ratios or vice versa, whichever is deemed more favourable. This was also hinted at by the results of Behera and Parhi (2016), who reported that increasing concentration beyond 0.4 mol L^{-1} had little to no effect when S/L =1% and T =35 °C, but the effect of concentration was not probed further. They also tested different S/L ratios (1, 3 and 5%) while keeping other factors constant (c =0.4 mol L^{-1}, T =35 °C), and found that Nd leaching efficiency decreased from 100 to 88% with increasing S/L ratio. This of course could have been countered by the use of higher concentration.

The average effect of time appeared to be of the same magnitude as concentration and S/L ratio. Leaching recovery of Nd increased 18 pp on average from 1 to 6 h and the factor showed no interaction with neither concentration nor S/L ratio but did interact with temperature. Leaching efficiencies grew with both increasing time and temperature, but the effect of time was more minor within the experimental domain. Because the effect of temperature was so much greater, the average effect of time diminished with increasing temperature from 29 to 8 pp, which is seen in the interaction plot (Fig. 2b).

Temperature appeared as the most prominent factor within the experimental domain with an average effect of 50 pp and the factor showed interaction with all of the other factors. The interaction with concentration is due to chemical potential and thermodynamic activity being functions of temperature. Little difference is observed on average between the two concentration levels at low temperature (7 pp), but a noticeable difference can be seen at high temperature (25 pp). The same is true for the S/L ratio with the higher absolute amount of acid at a low S/L ratio being affected more by the increasing temperature than at a

high S/L ratio. Behera and Parhi (2016) did not find as great of a difference within the temperature range they tested (35–80 °C) with leaching efficiency increasing from 92 to 100% after 4 h of leaching. The lesser difference observed can in part be explained by the more narrow range, and on the other hand likely due to the smaller overall particle size (46–180 μm) used in their work, requiring less time to leach in all conditions, damping the difference observed in the present work.

Overall judging by the results it would indeed appear that no true optimum exists, but rather multiple avenues to complete Nd dissolution with some constraints that ought to be taken into account when selecting leaching conditions. Using even very low acetic acid concentrations is viable if compensated for with a sufficiently low solid-to-liquid ratio to provide enough acid and protons for the leaching reaction. Similarly, using a more concentrated acetic acid allows for higher S/L ratios. Time and temperature feature a similar relationship, for we showed that complete Nd dissolution will occur in 24 h even at room temperature, but is equally possible within 1 h using high enough of a temperature (50–80 °C).

Similar results were reported by Gergoric et al. (2018), who achieved >95% leaching efficiencies for Nd when c =1.0 mol L^{-1}, S/L =1/50 g mL^{-1}, T =25 °C and stirring speed 400 min^{-1}. They tested lower acid concentrations as well, but leaching efficiency for 0.4 mol L^{-1} acetic acid was <75%, which in the light of our findings was likely due to the higher S/L ratio used. Yoon et al. (2015) didn't focus on the leaching aspect in their work but reported a Nd leaching efficiency of 94.2% in the conditions of their choosing (c =1.0 mol L^{-1}, S/L =1%, T =90 °C, t =3 h). Direct comparisons should be made with caution though because both of them leached roasted and oxidised NdFeB powders.

3.4. Leaching kinetics

The initial experiments showed complete dissolution of the magnet powder is possible at room temperature given enough time (24 h), but results from the main effect study saw leaching efficiencies reach a maximum of 60%, raising the question of how long is enough. Additionally, kinetic modelling can provide a better understanding of the leaching process and help with decision-making related to process design, for which reasons the kinetics experiment was undertaken.

Results obtained from the kinetics experiment for neodymium and iron were plotted against time, producing Fig. 3a. Initially, leaching appears to proceed linearly with recovery surpassing 80% after 12 h for both elements, after which the reaction slows down by a fair amount but eventually reaches 100% after 24 h. Reaction slowing down is likely due to the fairly broad particle size distribution (1–500 μm) with the remaining larger particles leaching slower after the depletion of smaller ones, reflecting the particle size distribution presented in Fig. 1b. The final samplings at 40 h feature a slight reduction in recovery for both elements, which resulted from the onset of iron precipitation.

The applicability of shrinking core models (SCMs), which are among the most popular models used for modelling heterogeneous solid-liquid reactions in hydrometallurgy (Othusitse and Muzenda, 2015), for describing the present leaching process was tested using results from the aforementioned experiment. Equation (4) was used to calculate the fraction of leached neodymium at each point in time.

$$X = \frac{\text{Nd leaching efficiency}}{100\ \%} \tag{4}$$

$$kt = 1 - (1 - X)^{\frac{1}{3}} \tag{5}$$

$$kt = 1 - \frac{2}{3}X - (1 - X)^{\frac{2}{3}} \tag{6}$$

The obtained values were fitted to two different models: equation (5) describes the shrinking core model, in which the rate of reaction is controlled by the surface chemical reaction, whilst equation (6) is used for the shrinking sphere model, where the reaction rate is controlled by diffusion (Othusitse and Muzenda, 2015). Fits for both models were done using the data points up to 24 h from the leaching experiment, plots of which are presented in Fig. 3b. The diffusion controlled model (6) appears to have a better fit statistically ($R^2 = 0.99041$), but the data points clearly show some curvature at the lower end of the graph. The chemically controlled model (5) has a slightly worse fit ($R^2 = 0.98470$) despite the data points showing a more linear trend excluding the deviations at the higher end. Based on these results it's impossible to give a definitive statement, but the findings of Behera and Parhi (2016) strongly point toward the reaction being chemically controlled. The leaching reaction happening on the surface of shrinking magnet particles would mean that grinding the magnets into a finer powder will further speed up the leaching reaction.

Table 5
Results of the iron precipitation experiments expressed as the precipitation efficiencies of Fe and Nd, in varying reaction conditions (temperature, time, pH).

No.	Aeration	T	t	pH	Precip. eff.	
		(°C)	(h)		Fe (%)	Nd (%)
1	Yes	30	2	5.0	15	8
2	Yes	30	6	5.0	63	17
3	Yes	80	2	5.0	99	5
4	Yes	80	6	5.1	99	8
5	No	90	2	4.2	49	6
6	No	90	6	4.2	72	14
7	No	90	2	5.0	73	6
8	No	90	6	5.0	86	5
9	Yes	90	2	3.9	84	7
10	Yes	90	6	4.0	96	7
11	Yes	90	2	5.0	95	5
12	Yes	90	6	5.0	96	9

3.5. Iron precipitation

3.5.1. Selection of precipitation agent

Since the oxidation of iron is possible using a variety of oxidants, oxidation-precipitation of iron from the PLSs was first attempted using three different approaches. Though to avoid the introduction of alien elements into the leaching solutions, the oxidation methods chosen were hydrogen peroxide, ambient air and aeration.

Initially, tests were run at room temperature but did not produce any good results. Further testing was conducted at elevated temperatures, for successful oxidation-precipitation of iron as goethite/magnetite from nickel-rich leach liquors at a temperature of 95 °C had been reported (Han et al., 2016). Secondly, it was found that H_2O_2 did not work for this application as it experienced rapid decomposition upon introduction into the PLS and did not have the chance to properly oxidise the iron(II) ions. This could be due to 'high' pH (>4), temperature and concentration of transition metals (Fe, Co, Ni). Another reason could be part of the H_2O_2 reacting with acetic acid to form peracetic acid. Even with periodical additions of fresh H_2O_2 over extended periods of time, no appreciable amounts of precipitate formed.

Oxidation at an elevated temperature in ambient air as well as the use of aeration proved most successful for precipitating iron selectively from the PLS. Partially covered sample solutions were placed on hotplate stirrers set to 95 °C and 800 min^{-1} and left for 24 h. Sample solutions had their pH adjusted to and maintained at 5 with periodical additions of dilute NaOH. Both methods managed to precipitate the majority of iron while retaining most of the neodymium in the solution.

3.6. Aeration experiments

A variety of precipitation experiments were conducted in small batches to study the viability of various reaction conditions and the influence of major factors such as time, temperature, pH and aeration. The most relevant experiments and findings are presented in Table 5.

Table 6
Mean elemental composition (wt.%) of the iron precipitates as determined quantitatively by ICP-OES and semi-quantitatively by SEM-EDS. Dysprosium was unable to be determined with EDS due to overlapping peaks of Fe and Dy, and boron due to the use of a boron viewing window.

	Fe	Nd	Pr	Ni	Dy	Co	B	Al	Tb	O	C	Σ
ICP	57.42	1.38	0.16	0.45	0.19	0.42	0.43	0.30	0.00	–	–	60.74
EDS	64.61	1.10	0.16	0.66	–	1.56	–	0.72	0.00	27.75	1.65	99.60

These results showed that major increases in iron precipitation are achieved by using aeration over passive ambient oxygen dissolution. While ambient air oxidation appeared possible, it would most certainly be unfeasible in any industrial scale application. Introducing aeration and small air bubbles into the solution increases the surface area available for oxygen dissolution by orders of magnitude. The other major factor appeared to be temperature. Increasing temperature allowed for a shorter reaction time by speeding up the oxidation process but it also carries a negative effect as oxygen's solubility in water decreases. This can be seen by comparing the Fe precipitation efficiencies achieved at 80 and 90 °C, where the increase in temperature has resulted in a minor reduction in Fe precipitation efficiency. Adjusting pH to 5 instead of 4 appeared to allow for a shorter reaction time without causing any additional Nd co-precipitation. The reason for this behaviour is that air oxidation is slower in acidic conditions and speeds up as pH increases (Kroschwitz et al., 2001). An alternative to aeration and air oxidation would be to use other oxidants, which could potentially increase oxidation efficiency and speed, but also incur additional costs (Khatri et al., 2017). This would also introduce alien elements into the solution, potentially complicating further processing and waste treatment.

The effect of acidity was further investigated with a set of experiments featuring incremental increases in pH, ranging from 5 to 8. Other factors were set to T =90 °C, t =2 h, ω =800 min^{-1} with aeration on. Results from this set showed that any increase in pH beyond 5 resulted in considerable and rapidly increasing co-precipitation of neodymium and other elements (see SI 5). Sample solutions with pH 7 and above were virtually devoid of metals, containing only boron. These findings would lead to believe that any further optimisation should be conducted at or below pH 5. Our experiments showed that 96–99% of iron could be precipitated while retaining 91–95% of neodymium in solution when using the aeration method and precipitating at 80–90 °C, pH 5 and for at least 2 h. These results are on par with those of Yoon et al. (2015), who achieved 99% separation of iron and 94.2% recovery for neodymium.

Improvements in precipitation efficiency and rate could likely be found using proper aeration equipment and control. Another possibility is the use of even higher temperatures under increased pressure, but that would also necessitate the use of some other form of oxidation. Neodymium losses on the other hand could possibly be decreased by using filtration for separation, which would require some form of flocculant to be added, but allow washing of the iron precipitate.

3.7. Characterization of precipitate

To assess the selectivity of the precipitation reaction and composition of the formed precipitate, three replicate sample solutions were prepared and iron was precipitated using the aeration method in the conditions of T =90 °C, t =2 h, ω =800 min^{-1}. The composition of the formed precipitates was examined using ICP-OES, SEM-EDS and PXRD. The elemental compositions obtained from ICP and EDS analyses are presented in Table 6. Judging by the ICP-OES results, the precipitates appeared reasonably pure, as impurities accounted for 3.3% of the total mass of the obtained precipitates. REEs in total constituted 1.72% of the precipitates, of which the majority (1.38%) was neodymium. Iron content was 57% of total mass and 95% of precipitated elements. Almost 40% of the total mass went undetected by the ICP-OES analysis, presumably due to the remainder being oxygen and hydrogen.

All three measured samples produced nearly identical PXRD patterns. The search-match phase analyses made with the patterns resulted congruently in the identification of an orthorhombic FeO(OH) phase without the presence of other crystalline phases, as no unassigned diffraction peaks remained in the patterns (see SI 6 for further details). Pure FeO(OH) would consist of Fe 62.85%, O 36.01% and H 1.13% by mass. Iron concentrations determined with ICP-OES differ from these values somewhat, which is in part explained by the contained impurities. It is also possible that the precipitate contains minor amounts of other iron oxides or oxide-hydroxides, as was the case when Han et al. (2016) precipitated iron from nickel-rich leach-liquors, but which went undetected due to low concentration and the amorphous nature of our precipitates. Further optimisation of the precipitation conditions could potentially reduce the co-precipitation of REEs and other elements. Improvements might be found using lower pH and allowing longer reaction times instead.

4. Conclusions

The present work has demonstrated that no one optimal condition exists for the recovery of neodymium from NdFeB magnets by acetic acid leaching. The novel feature of the present work was the multivariate investigation of the major factors influencing the leaching process, which has shown that up to 100% of Nd could be dissolved using a wide variety of different conditions. High leaching efficiencies have been reported in the previous work, but only in a specific set of conditions (Behera and Parhi 2016). The present work shows that there is room for adjustment of the individual factors. Concentration and S/L ratio as well as time and temperature act as pairs of factors, where changes in the other can be compensated for by changing the other. Increasing temperature can also facilitate the usage of lower concentrations or higher S/L ratios due to their interactions. Information provided in the present work should help any potential application of acetic acid for the leaching of waste NdFeB magnets, and with the upscaling of the said process as no specific set and narrow range of variables has to be strictly followed.

Secondly, as a novel application, it was shown that dissolved iron could be effectively separated from the acetic acid leachate as iron(III) oxide-hydroxide by oxidative precipitation with low levels of neodymium co-precipitation. At best (pH = 5, T =80 °C, t =2 h) the efficiency of iron removal was 99%, while only 5% neodymium was lost in the process due to co-precipitation. Oxidation of iron(II) was achieved by simple and inexpensive aeration. Results obtained using this method are on par with the approach of oxidative roasting and selective leaching (Yoon et al., 2015), and achievable in a similar time frame but at a much lower temperature. As iron(III) precipitates at a fairly low pH, no excessive use of neutralising reactants is required. In fact, the pH of the PLS post-leaching was found to be high enough as is, making precipitation possible, albeit slower, without the use of neutralising agents entirely. Separation of iron from the PLS enables the production of more pure REE products by e.g. the oxalate precipitation method or liquid-liquid extraction, which are known to suffer from the presence of iron to an extent.

Declaration of competing interest

The authors declare that they have no known competing financial interests or personal relationships that could have appeared to influence the work reported in this paper.

Acknowledgements

The work was supported by the Department of Chemistry at the University of Jyväskylä, and the experimental work received funding from the European Regional Development Fund (grant number: A76928). Hannu Salo is gratefully acknowledged for SEM-EDS imaging and analysis. Green Disposal Oy, Ltd is acknowledged for providing the waste NdFeB magnets.

Appendix A. Supplementary data

Supplementary data to this article can be found online at https://doi.org/10.1016/j.clet.2022.100544.

References

Behera, S.S., Panda, S.K., Mandal, D., Parhi, P.K., 2019. Ultrasound and Microwave assisted leaching of neodymium from waste magnet using organic solvent. In: Hydrometallurgy, 185, pp. 61–70. https://doi.org/10.1016/j.hydromet.2019.02.003.

Behera, S.S., Parhi, P.K., 2016. Leaching kinetics study of neodymium from the scrap magnet using acetic acid. In: Sep. Purif. Technol., 160, pp. 59–66. https://doi.org/10.1016/j.seppur.2016.01.014.

Binnemans, K., Jones, P.T., Blanpain, B., Van Gerven, T., Yang, Y., Walton, A., Buchert, M., 2013. Recycling of rare earths: a critical review. In: J. Cleaner Prod., 51, pp. 1–22. https://doi.org/10.1016/j.jclepro.2012.12.037.

Brown, D., Ma, B.-M., Chen, Z., 2002. Developments in the processing and properties of NdFeb-type permanent magnets. In: J. Magn. Magn. Mater., 248, pp. 432–440. https://doi.org/10.1016/S0304-8853(02)00334- 7.

Corbetta, G., 2015. Wind Energy Scenarios for 2030. European Wind Energy Association.

Cullity, B.D., Graham, C.D., 2009. Introduction to Magnetic Materials, second ed. Wiley, Hoboken, NJ, USA, pp. 477–504. isbn: 978-0-471-47741-9.

Degen, T., Sadki, M., Bron, E., König, U., Nénert, G., 2014. The HighScore suite. In: Powder Diffr, 29, pp. S13–S18. https://doi.org/10.1017/S0885715614000840. S2.

Erust, C., Akcil, A., Tuncuk, A., Deveci, H., Yazici, E.Y., 2021. A multi-stage process for recovery of neodymium (Nd) and dysprosium (Dy) from spent hard disc drives (HDDs). In: Miner. Process. Extr. Metall. Rev., 42, pp. 90–101. https://doi.org/10.1080/08827508.2019.1692010, 2.

Firdaus, M., Rhamdhani, M.A., Durandet, Y., Rankin, W.J., McGregor, K., 2016. Review of high-temperature recovery of rare earth (Nd/Dy) from magnet waste. In: J. Sustain. Metall., 2, pp. 276–295. https://doi.org/10.1007/s40831-016-0045-9.

Forti, V., Baldé, C.P., Kuehr, R., Bel, G., 2020. The Global E-Waste Monitor 2020: Quantities, Flow, and the Circular Economy Potential. United Nations University (UNU)/United Nations Institute for Training and Research (UNITAR) - co-hosted SCYCLE Programme, International Telecommunication Union (ITU) & International Solid Waste Association, Bonn/Geneva/Rotterdam.

Free, M.L., 2013. Hydrometallurgy: Fundamentals and Applications, first ed. Wiley-TMS, Weinheim, Germany, pp. 212–213. isbn: 978-1-118-23077-0.

Gates-Rector, S., Blanton, T., 2019. The Powder Diffraction File: a quality materials characterization database. In: Powder Diffr, 34, pp. 352–360. https://doi.org/10.1017/S0885715619000812, 4.

Gergoric, M., Ravaux, C., Steenari, B.-M., Espegren, F., Retegan, T., 2018. Leaching and recovery of rare- earth elements from neodymium magnet waste using organic acids. In: Metals (Basel), 8. https://doi.org/10.3390/met8090721, 9.

Gislev, M., Grohol, M., 2018. Report on critical raw materials and the circular economy. European Commission. https://doi.org/10.2873/167813.

Habib, K., Wenzel, H., 2014. Exploring rare earths supply constraints for the emerging clean energy technologies and the role of recycling. In: J. Cleaner Prod., 84, pp. 348–359. https://doi.org/10.1016/j.jclepro.2014.04.035.

Han, H., Sun, W., Hu, Y., Cao, X., Tang, H., Liu, R., Yue, T., 2016. Magnetite precipitation for iron removal from nickel-rich solutions in hydrometallurgy process. In: Hydrometallurgy, 165, pp. 318–322. https://doi.org/10.1016/j.hydromet.2016.01.006.

Itoh, M., Miura, K., Machida, K.-i., 2008. Novel rare earth recovery process on Nd-Fe-B magnet scrap by selective chlorination using NH_4Cl. In: J. Alloys Compd., 477, pp. 484–487. https://doi.org/10.1016/j.jallcom.2008.10.036.

Kaya, M., 2019. Electronic Waste and Printed Circuit Board Recylcing Technologies. Springer, Cham, Switzerland. https://doi.org/10.1007/978-3-030-26593-9 isbn: 978-3-030-26593-9.

Khatri, N., Tyagi, S., Rawtani, D., 2017. Recent strategies for the removal of iron from water: a review. In: Journal of Water Process Engineering, 19. https://doi.org/10.1016/j.jwpe.2017.08.015, 291–34.

Imaging technology to lanthanides. In: Kroschwitz, J.I., Howe-Grant, M. (Eds.), 2001, Kirk-Othmer Encyclopedia of Chemical Technology, fourth ed., ume 14. Wiley, New York, NY, USA, pp. 411–445. isbn: 0-471-52683-5.

Li, L., Dunn, J.B., Zhang, X.X., Gaines, L., Chen, R.J., Wu, F., Amine, K., 2013. Recovery of metals from spent lithium-ion batteries with organic acids as leaching reagents and environmental assessment. In: J. Power Sources, 233, pp. 180–189. https://doi.org/10.1016/j.jpowsour.2012.12.089.

Liu, F., Porvali, A., Halli, P., Wilson, B.P., Lundström, M., 2020a. Comparison of different leaching media and their effect on REEs recovery from spent Nd-Fe-B magnets. In: JOM, 72, pp. 806–815. https://doi.org/10.1007/s11837-019-03844-7, 2.

Liu, F., Porvali, A., Wang, J., Wang, H., Peng, C., Wilson, B.P., Lundström, M., 2020b. Recovery and separation of rare earths and boron from spent Nd-Fe-B magnets. In: Miner. Eng., 145, 106097. https://doi.org/10.1016/j.mineng.2019.106097.

Mineral Commodity Summaries 2021, 2021. U.S. Geological Survey. https://doi.org/10.3133/mcs2021.

Önal, M.A.R., Borra, C.R., Guo, M., Blanpain, B., Van Gerven, T., 2017. Hydrometallurgical recycling of NdFeB magnets: complete leaching, iron removal and electrolysis. In: J. Rare Earths, 35, pp. 574–584. https://doi.org/10.1016/S1002-0721(17)60950-5, 6.

Orefice, M., Binnemans, K., Vander Hoogerstraete, T., 2018. Metal coordination in the high-temperature leaching of roasted NdFeB magnets with the ionic liquid betainium bis(trifluoromethylsulfonyl)imide. In: RSC Adv, 8, pp. 9299–9310. https://doi.org/10.1039/C8RA00198G, 17.

Othusitse, N., Muzenda, E., 2015. Predictive models of leaching processes: a critical review, 26th–27th Nov. 2015. In: 7th International Conference of Latest Trends in Engineering & Technology (ICLTET'2015). Irene, Pretoria, South Africa. https://doi.org/10.15242/IIE.E1115039.

Parhi, P.K., Sethy, T.R., Rout, P.C., Sarangi, K., 2016. Separation and recovery of neodymium and praseodymium from permanent magnet scrap through the hydrometallurgical route. Philadelphia, PA, U. S.. In: Sep. Sci. Technol., 51, pp. 2232–2241. https://doi.org/10.1080/01496395.2016.1200087, 13.

Rademaker, J.H., Kleijn, R., Yang, Y., 2013. Recycling as a strategy against rare earth element criticality: a systemic evaluation of the potential yield of NdFeB magnet recylcing. In: Environ. Sci. Technol., 47, pp. 10129–10136. https://doi.org/10.1021/es305007w, 18.

Riaño, S., Binnemans, K., 2015. Extraction and separation of neodymium and dysprosium from used NdFeB magnets: an application of ionic liquids in solvent extraction towards the recycling of magnets. In: Green Chem, 17, pp. 2931–2942. https://doi.org/10.1039/C5GC00230C, 5.

Sáenz-Galindo, A., Castañeda-Facio, A.O., Rodríguez-Herrera, R. (Eds.), 2021. Green Chemistry and Applications, first ed. CRC Press, Boca Raton, FL, USA. isbn: 978-0-367-26033-0.

Sagawa, M., Hirosawa, S., Yamamoto, H., Fujimura, S., Matsuura, Y., 1987. Nd–Fe–B permanent magnet materials. In: Jpn. J. Appl. Phys., 26, pp. 785–800. https://doi.org/10.1143/jjap.26.785, 6.

Sim, J.H., Kamaruddin, A.H., Long, W.S., Najafpour, G., 2007. Clostridium aceticum—a potential organism in catalyzing carbon monoxide to acetic acid: application of response surface methodology. In: Enzyme Microb. Technol., 40, pp. 1234–1243. https://doi.org/10.1016/j.enzmictec.2006.09.017, 5.

Yang, Y., Walton, A., Sheridan, R., Güth, K., Gauß, R., Gutfleisch, O., Buchert, M., Steenari, B.-M., Gerven, T.V., Jones, P.T., Binnemans, K., 2017. REE recovery from end-of-life NdFeB permanent magnet scrap: a critical review. In: J. Sustain. Metall., 3, pp. 122–149. https://doi.org/10.1007/s40831-016-0090-4, 1.

Yoon, H.-S., Kim, C.-J., Chung, K.W., Jeon, S., Park, I., Yoo, K., Jha, M.K., 2015. The effect of grinding and roasting conditions on the selective leaching of Nd and Dy from NdFeB magnet scraps. In: Metals (Basel), 5. https://doi.org/10.3390/met5031306, 3.